Blends of Polyamide1010 with Unmodified and Maleic-Anhydride-Grafted High-Impact Polystyrene

GUANGXIN CHEN, JINGJIANG LIU

Polymer Physics Laboratory, Changchun Institute of Applied Chemistry, Chinese Academy of Sciences, Changchun, 130022

ABSTRACT: The crystallization behaviors, dynamic mechanical properties, tensile, and morphology features of polyamide1010 (PA1010) blends with the high-impact polystyrene (HIPS) were examined at a wide composition range. Both unmodified and maleic-anhydride-(MA)-grafted HIPS (HIPS-*g*-MA) were used. It was found that the domain size of HIPS-*g*-MA was much smaller than that of HIPS at the same compositions in the blends. The mechanical performances of PA1010–HIPS-*g*-MA blends were enhanced much more than that of PA1010–HIPS blends. The crystallization temperature of PA1010 shifted towards higher temperature as HIPS-*g*-MA increased from 20 to 50% in the blends. For the blends with a dispersed PA phase ($\leq$35 wt %), the T_c of PA1010 shifted towards lower temperature, from 178 to 83°C. An additional transition was detected at a temperature located between the T_g's of PA1010 and PS. It was associated with the interphase relaxation peak. Its intensity increased with increasing content of PA1010, and the maximum occurred at the composition of PA1010–HIPS-*g*-MA 80/20. © 1999 John Wiley & Sons, Inc. J Appl Polym Sci 74: 857–865, 1999

Key words: polyamide1010; high-impact polystyrene; maleic anhydride

INTRODUCTION

Polyolefins are often used to blend with engineering thermoplastics (e.g., polyamides or polyesters) to prepare blend and alloys with a combination of properties unattainable in any single polymer. In practice, however, it is difficult to obtain good performance because they are incompatible. Therefore, studies aimed at enhancing the compatibility between them have been carried out by many investigators. These works have studied the use of functionalized polyolefins as a compatibilizer. The functional monomers, which can interact with the amino in polyamides (PAs) or hydroxyl groups in polyesters, are introduced in polyolefins through an appropriate copolymeriza-tion method. Various functional monomers, such as maleic anhydride, methacrylic acid, acrylic acid, glycidyl methacrylate, and sulfonic acid have been successfully used in this way to compatibilize the systems of PA6–polystyrene (PS),[1–4] PA6–acylonitrile–butadiene–styrene (ABS),[5–8] PA6–polypropylene (PP),[9] PA1010–PP,[10] PA6–PE,[11] PBT–HIPS,[12] PBT–PS,[13] and PET–ABS.[14]

However, few research works have been carried out on the blend of HIPS and PA1010. In general, this blend system is of scientific and commercial significance as well-known HIPS is a commercial product in large use. It has been used to manufacture the inner boxes of refrigerators and TV housings throughout the world. However, HIPS liners could meet problems in terms of the environment friendly blowing agents, HCFC-141b, from rigid polyurethane foam used for the insulation of domestic refrigerators and freezers.

Taking into consideration the ozone depletion potential and global warming potential, the 1990 revision of the Montreal protocol calls for the phase out of CFC-11 by January 1, 2000; and, as well known today, there is wide acceptance that HCFC-141b is the ideal substitute for CFC-11 replacement. At an early stage of the work to develop appliance foam system blown with HCFC-141b, it was recognized that the greater solvent power of the material compared with CFC-11 could create problems in terms of liner attack. The HIPS lines, in contact with HCFC-141b blown foam, showed a tendency to exhibit multiple crazes, softened, and blistered. A new objective of the work was to investigate the foam/ liner interactions and ultimately to develop a HCFC-141b compatible liner.

It was considered that the most convenient and cost effective solution would be to improve the HCFC-141b resistance of current HIPS materials through modification of the chemical composition, morphology, and additives, while another way would be to laminate with a barrier layer on the foam contact surface. Polyamides have excellent solvent resistance, and they exhibit superior barrier performance. PA1010 is the best one in nylon family by blending with HIPS. Its cost is lower comparing with PA11 and PA12 and its processing temperature matched with HIPS comparing with PA6 and PA66. HIPS may undergo decomposition during blending it with PA6 or PA66 because their melting temperatures are over 250°C. The compatibilized blends of HIPS and PA1010 have been used to manufacture the liners of refrigerators and freezers with HCFC-141b blowing agent successfully in China. From the scientific point of view, it is necessary to highlight the relationship among the miscibility, the effect of compatibilizer, and the morphology and mechanical properties of the blends of HIPS and PA1010. This is the main purpose of our research work. Both PA1010–HIPS and PA1010–HIPS-g-MA blends with wide range of composition were investigated.

EXPERIMENTAL

Materials

HIPS was a commercial product containing 7% polybutadiene (492-J) manufactured by Yanshan Petrochemical Co. Beijing, China. Its melting flow rate (MFR) is 2.6 g/10 min. PA1010 was supplied from Jilin Shijinggou Union Chemical Co., China. Its relative viscosity is 2.1, and MFR is 10 g/10 min.

Preparation of Compatibizer and Blends

HIPS-g-MA was prepared by melt-mixing of HIPS and maleic anhydride (MA) at 180°C initiated by dicumyl peroxide (DCP) in a Brabander mixing chamber. The content of MA in HIPS-g-MA was 4.7 wt %. The grafting degrees were determined by the chemical titration method.

PA1010 was dried for 24 h at 90°C before melt-blending. Binary PA1010–HIPS and PA1010–HIPS-g-MA blends were prepared by melt mixing using a Brabender twin-screw extruder operating at a rotation speed of 20 rpm and mixing temperature designed as 210–235°C. Compositions of PA–HIPS (or HIPS-g-MA) had weight ratios of 90/10, 80/20, 65/35, 50/50, 35/65, and 20/80.

Crystallization and Thermal Analysis

The thermal behavior of the blend samples was determined on a Perkin–Elmer DSC-7. The fusion thermogram was obtained from 50 to 220°C at a heating rate of 20°C/min. All measurements were performed under a nitrogen atmosphere.

Dynamic Mechanical Analysis

DMA data, storage modules E', and tan δ, were determined at 3.5 Hz using a Rheovibron DDV-II-EA dynamic mechanical viscoelastometer.

Morphological Observation

The morphology of blends was observed with a scanning electron microscope (SEM; JXA-840) at an accelerating voltage of 25 KV. The blend samples were fractured at liquid nitrogen temperature, and the cryogenically fractured samples etched for 2 h to increase the contrast.

Tensile Properties

Dumbbell-shaped specimens were prepared at 230°C with hot-press molding. The tensile tests were carried out on an Instron 1121 machine at room temperature with a crosshead speed of 5 mm/min. Five specimens of each blend were tested, and the average values were taken as the experimental data.

RESULTS AND DISCUSSION

Crystallization and Thermal Analysis

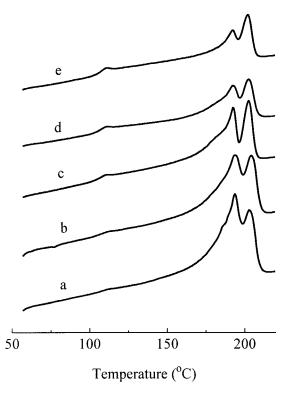The differential scanning calorimetric (DSC) thermograms of PA1010–HIPS and PA1010–

molecular chains effectively. The DSC cooling curves of blends of PA1010 with HIPS and HIPS-g-MA are shown in Figures 3 and 4, respectively.

Figure 3 shows the thermograms of PA1010–HIPS blends with various compositions. The T_c of PA1010 in PA1010–HIPS blends remained constant. However, in the PA1010–HIPS-g-MA blends, as shown in Figure 4, the crystallization temperature of PA1010 shift towards higher temperature as the content of HIPS-g-MA in the blends increased from 20 to 50%. Taking into account an experimental error of the DSC results (about 1°C), it is tentatively suggested that HIPS-g-MA acts as a nucleating agent in the PA1010 crystallization process. For the blends with a dispersed PA phase (≤ 35 wt %), the T_c of PA1010 shift towards lower temperature from 178 to 83°C. This so-called fractionated crystallization is observed. The described effects, in particular, the fractionation of the crystallization, depend to a large extent on the dispersion of the minor component. With increasing dispersivity of that component, the magnitudes of its additional crystallization peaks become stronger at the expense of the usual peak.
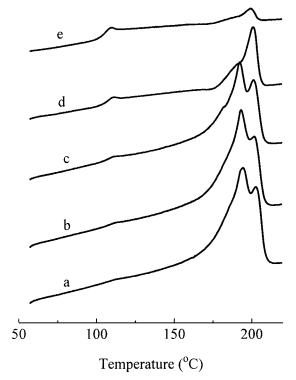

Figure 1 DSC thermograms of PA1010–HIPS blends: (a) 80/20; (b) 65/35; (c) 50/50; (d) 35/65; (e) 20/80.

HIPS-g-MA are shown in Figures 1 and 2, respectively. In the PA1010–HIPS blend system, the T_m of PA1010 in blends remained constant with increasing HIPS. As shown in Figure 2, the heat of fusion of lower temperature of PA1010 decreased as HIPS-g-MA increased, and the T_m of PA1010 is unaffected by adding HIPS-g-MA. This feature suggests that some chemical reactions occur between MA groups in HIPS-g-MA and the terminal amino group of PA1010 in the PA1010–HIPS-g-MA blend as follows:

The number of hydrogen bond in PA1010 phase would decrease owing to the chemical reaction. The big amide groups formed *in situ* between terminal amino group in PA1010 and MA groups in HIPS-g-MA can inhibit the folding of PA1010

Figure 2 DSC thermograms of PA1010–HIPS-g-MA blends: (a) 80/20; (b) 65/35; (c) 50/50; (d) 35/65; (e) 20/80.
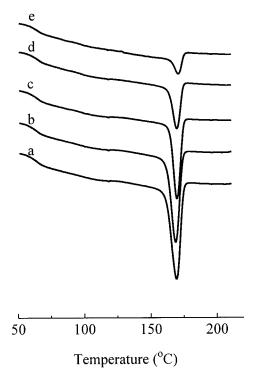
Figure 3 DSC crystallization exotherms of PA1010–HIPS blends: (a) 80/20; (b) 65/35; (c) 50/50; (d) 35/65; (e) 20/80.

The fractionated crystallization is characteristic for the crystallization behavior of a semicrystalline polymer blended with an incompatible polymer. This phenomenon has been observed so far in block copolymers comprising PEO–PE–PEO and PEO–PS[15,16] and in blends comprising PE–PS,[17] PP–SBS,[18] PE–POM,[19] PVDF–PA6,[20] PVDF–PA66, PA6–PP,[21] PE–PP, PBT–PC,[22] and PA–ABS[23] when the crystallizable component is included in the noncrystallizable matrix in fine dispersed domains. The smaller the particles, the more distinct the effect.

Among a large amount of small polymer droplets, each of volume V_D, the fraction of droplets containing exactly Z heterogeneities of the kind "1" that initially induced crystallization follows a Poisson distribution function.[24] It reads,

$$f_z^{(1)} = [(M^{(1)}V_D)^Z/Z!]\exp[-M^{(A)}V_D] \qquad (1)$$

where $M^{(1)}$ is the concentration of randomly suspended heterogeneities, and $M^{(1)}V_D$ is their mean number per droplet. The fraction of droplets containing at least one heterogeneity of the kind "1" is given by $f_{z>0}^{(1)} = 1 - f_0^{(1)}$ and amounts to

$$f_{z>0}^{(1)} = 1 - \exp[-M^{(1)}V_D] \qquad (2)$$

The consideration of a droplet size distribution may somewhat modify this equation. $f_{z>0}^{(1)}$ describes that part of the droplets and, therefore, of the material that crystallizes induced by heterogeneity "1". The remainder crystallizes at a greater undercooling degree induced by heterogeneity, "2", and so on. For these further crystallization steps, the same considerations hold. Since $f_{z>0}^{(i)}$ depends on V_D, the influence of the dispersitivity on the relative strength of the different crystallization steps is obvious. For sufficiently large droplets, $f_{z>0}^{(1)}$ is near unity, and no fractionated crystallization occurs. On the contrary, a certain crystallization step is suppressed (or undetectable) if the relation $M^{(i)}V_D \ll 1$ holds. From the relative intensity of the different crystallization steps, conclusions can be drawn on the concentration of the respective heterogeneities if the mean size of the droplets is known. From the results shown in Figures 3 and 4, we can conclude that the domain size, that is, V_D, in PA1010–
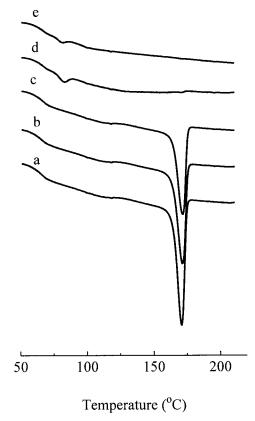

Figure 4 DSC crystallization exotherms of PA1010–HIPS-*g*-MA blends: (a) 80/20; (b) 65/35; (c) 50/50; (d) 35/65; (e) 20/80.
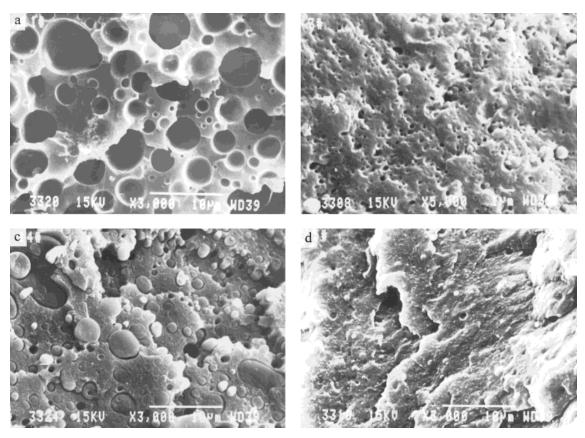
Figure 5 SEM photomicrographs of blends: (a) 65PA 1010–35HIPS; (b) 65PA 1010–35HIPS-*g*-MA; (c) 20PA 1010–80HIPS; (d) 20PA 1010–80HIPS-*g*-MA.

HIPS-*g*-MA (35/65 and 20/80) blends is small enough so that the fractionated crystallization in PA1010 phase was obviously detected. On the other hand, the fractionated crystallization of PA1010 domains in PA1010–HIPS blends cannot be observed at all. It is related to the larger volume of droplets in these blends. These results are shown with the micrographs of the samples in Figure 5.

Morphology generation during mixing of polymer components involves a balance between the competing processes of fluid drop breakup and coalescence. Taylor studied the deformation and disintegration of Newtonian fluids.[25,26] Tokita has derived an expression for describing the particle size of a dispersed phase in polymer blends.[26,27] At equilibrium, where breakup and coalescence are balanced, the equilibrium particle size D may be expressed as

$$D = (24P_r\nu/\pi\sigma_{12})(\Phi + 4P_rE\Phi^2/\pi\sigma_{12}) \quad (3)$$

where σ_{12}, ν, E, and P_r refer to stress field, interfacial tension, bulk breaking energy, and proba-

bility that a collision will result in coalescence, respectively. Equation (3) predicts that the equilibrium particle size decreases when the stress field becomes larger, the interfacial tension becomes smaller, and the volume fraction of the dispersed phase is smaller. As represented in Table I and Figure 5, because of the decrease of interfacial tension that resulted from the chemical reaction in the blend of PA1010–HIPS-*g*-MA, the average domain size was reduced to approximately one-twentieth of those in the uncompatibilized blend systems at the same composition. These results are in agreement with the trends predicted in eq. (3). The average volumes V_D of the dispersed PA1010 particles in the PA1010–HIPS-*g*-MA 35/65 and 20/80 blends are significantly smaller than those in the system of PA1010–HIPS, so that the relation $M^{(i)}V_D \ll 1$ holds, and the fractionated crystallization is observed.

Dynamic Mechanical Analysis

Figure 6 shows the temperature dependence of the storage modulus E', and loss factor tan δ for

Table I   Mean Particle Size of the Dispersed Phase

Blend	Mean Particle Size (μm)
PA1010–HIPS:	
80/20	4.0
65/35	4.2
50/50	co-continuous
35/65	2.9
20/80	1.7
PA1010–HIPS-g-MA:	
80/20	0.20
65/35	0.27
50/50	co-continuous
35/65	<0.2
20/80	0.1–0.05

the PA1010. Clearly, three well-defined relaxation peaks are observed. The mechanism of the relaxations resulting from the molecular motion has been investigated by a number of workers. For pure PA1010, three mechanical loss peaks, denoted as α, β, and γ, are shown in Figure 6. The maximum in tan δ, α relaxation, associated with the glass transition of the amorphous parts of PA1010 is localized near $T_\alpha = 67°C$, while the β and γ relaxation are found near -62.5 and $-130°C$, respectively, which are related to the mobility of the polar groups (—CONH—) and the excitation of cooperative motions in the methylene groups (—CH$_2$—) in the main chain, respectively.
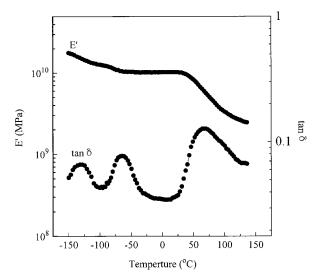

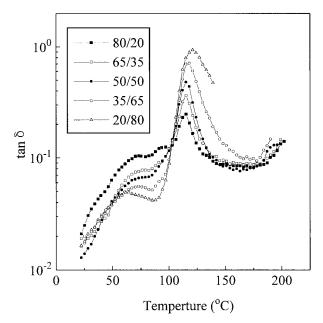**Figure 6**   DMA spectrum of PA1010.

Figure 7   DMA spectra of PA1010/HIPS blends.

While the miscibility of the blends can be speculated from the number of T_g's, the composition of the phases can be calculated adequately according to the Fox equation, with the T_g shift values for the partially miscible blends,

$$1/T_g = W_1/T_{g1} + W_2/T_{g2} \qquad (4)$$

The subscripts 1 and 2 refer to the pure components, and W refers to the weight fraction.

The results are given in Figures 7 and 8 in terms of the temperature dependence of the loss factor of PA1010–HIPS and PA1010–HIPS-g-MA blends at various compositions. A summary of the experimental investigations on the main relaxations is tabulated in Table II. The high-temperature transition of HIPS (T_g of PS) shifted towards lower temperatures can be seen with the decrease of HIPS content from 80 to 20% in PA1010–HIPS blends. The main relaxation of PA1010 shift towards higher temperatures. From these results, it may be inferred that the molecular segments of PA1010 and those of HIPS have migrated toward each other, especially when PA1010 forms the continuous phase. The partial miscibility between the components gets worse when HIPS is the matrix. The shifting degree inwards of the two T_g's is decreased. Another feature can be observed by comparing the dynamic mechanical analysis (DMA) spectra of PA1010–HIPS blends and PA1010–HIPS-g-MA
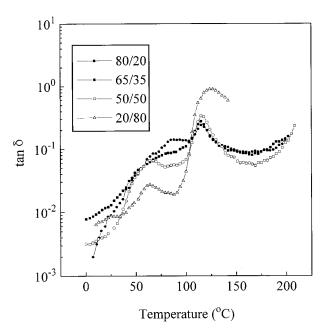
Figure 8 DMA spectra of PA1010–HIPS-g-MA blends.

blends. For PA1010–HIPS-g-MA blends, the intensities of T_g relaxation related to HIPS-rich phase are lowered. It can be inferred that plenty segments of HIPS have migrated to form the interface or to mix with PA1010 phase in the PA1010–HIPS-g-MA blends. The miscibility between the components in compatibilized blends is much better than that in the uncompatibilized ones. These conclusions are dealt with the observation by scanning electron microscopy (SEM), and they may be verified by the micrographs of these samples shown in Figure 5. For the PA1010–HIPS (20/80) blend, PA1010 is the dispersed phase, the sharp interface and the clear gaps between the domains and matrix are observed. On the other hand, these gaps are invisible in micrographs of PA1010–HIPS (65/35) blend and compatibilized blends.

An additional transition appears at a temperature located between the T_g's of PA1010 and PS. According to the well-known knowledge on polymer molecular motion, it is associated with interphase relaxation. The intensity of interphase relaxation peak increases with increasing content of PA1010, the intensities of interphase relaxation peaks are bigger in the blends of PA1010–HIPS-g-MA than those in the blends of PA1010–HIPS, and the maximum occurs at the composition of PA1010–HIPS-g-MA 80/20. It may be suggested that some interactions may exist between the PS

component of HIPS and PA1010. It is worth pointing out that the relaxation peaks related to interphases were measured in both of PA1010–HIPS 80/20 and PA1010–HIPS-g-MA blends instead of the shoulders in the other samples on the dynamic mechanical spectra. On the contrary, the interphase relaxation cannot be confirmed on the DMA spectra of PA1010–HIPS (20/80) and PA1010–HIPS-g-MA (20/80) blends and the interphase relaxation is responsible for the miscibility between the components in these blends. It seems of interest that the glass transition temperature of PA1010 (66.9°C) in PA1010–HIPS-g-MA (80/20) system is located at a lower temperature than that corresponding to the T_g of PA1010 (71.0°C) in the PA1010–HIPS (80/20) system (Fig. 9). On the one hand, T_g of PA1010 should increase because of the mixing of PS component. On the other hand, owing to the chemical reaction between the PA1010 and HIPS-g-MA, some hydrogen bonds in PA1010 were broken, and the molecular motion of PA1010 chains should occur at lower temperature. The results mentioned above are controlled by the competition between the two factors.

Tensile Properties

Interfacial adhesion is an important parameter for controlling the mechanical properties of multiphase systems; good adhesion between the matrix and dispersed phase may be essential for proper stress transfer without interfacial debonding. The tensile properties of PA1010–HIPS and

Table II Thermal Transition Parameters of the Blends

Blend	PA1010			HIPS T_g (PS) (°C)
	T_β (°C)	T_α (°C)	T_i (°C)	
PA1010–HIPS:				
80/20	−74	71.0	91.6	114.3
65/35	−74	71.5	—	114.9
50/50	−73	71.9	—	115.3
35/65	−74	71.2	—	116.8
20/80	−75	63.1	—	120.9
PA1010/HIPS-g-MA:				HIPS-g-MA:
80/20	−85	66.9	86.4	115.2
65/35	−87.5	—	—	115.4
50/50	−95	64.8	87.4	116.4
20/80	−80	63.2	—	124.9

PA1010–HIPS-*g*-MA samples are summarized in Table III. Compared with the unmodified blends, the tensile strength (σ), elongation at break (ε), and the energy to tensile failure (u) of modified blends were significantly improved. Perhaps the improved adhesion between PA1010 and HIPS-*g*-MA was due to the chemical linking *in situ*. These features can be tentatively explained that the HIPS-*g*-MA reacts with end-NH$_2$ groups of polyamide 1010 to form chemical linking, PA1010-*g*-HIPS, during reactive blending, providing efficient compatibility, reducing surface tension, decreasing dispersed phase size, and improving interfacial adhesion between PA1010 and HIPS-*g*-MA. As pointed out in previous work,[28] a graft copolymer stays preferentially on surfaces of dispersed domains, acting as an interfacial agent. The presence of such an interfacial agent would require less energy for breaking large dispersed particles during melt blending; hence, it enhances domains to adhere to the continuous phase.

CONCLUSIONS

Blends of polyamide 1010 with unmodified and maleic-anhydride-grafted high-impact polystyrene were investigated. HIPS-*g*-MA was expected to react with PA1010 in the molten state to provide interfacial bonding between the two phases. The
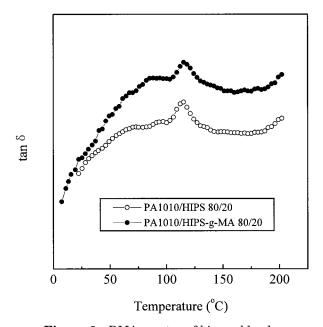

Figure 9 DMA spectra of binary blends.

Table III Tensile Properties of Binary Blends

Blend	σ (MPa)	U (J)	ε (%)	E (MPa)
PA1010–HIPS:				
80/20	35	0.44	18.7	792
65/35	35	0.19	9.9	740
50/50	33	0.12	8.0	897
35/65	21	0.02	2.5	955
20/80	22	0.02	2.3	1008
PA1010–HIPS-*g*-MA:				
80/20	43	1.24	43.1	675
65/35	48	0.85	27.7	860
50/50	51	0.42	15.0	1030
35/65	33	0.07	4.8	1048
20/80	32	0.05	3.8	849

HIPS-*g*-MA significantly changed the morphology and mechanical properties of the blends as compared with HIPS. This is attributed to the MA group of HIPS-*g*-MA reacting with the terminal-NH$_2$ group of PA. A graft copolymer, PA1010-*g*-HIPS, was synthesized. It is an effective compatibilizer in these blends, and, consequently, the interfacial tension between the two phases is decreased. The crystallization temperature of PA1010 shifts towards higher temperature as HIPS-*g*-MA increased from 20 to 50% in the blends; and for the blends with a disperse PA phase ($\leq$35 wt %), the T_c of PA1010 shifts towards lower temperature from 178 to 83°C. From the results of DMA, a new interphase relaxation peak appears at a temperature, which is located between the T_g's of PA1010 and PS in both systems.

REFERENCES

1. Ide, F.; Hasegawa, A. J Appl Polym Sci 1974, 18, 963.
2. Chen, C. C.; Fortan, E.; Min, K. E.; White, J. L. Polym Eng Sci 1988, 28, 69.
3. Park, I.; Barlow, J. W.; Paul, D. R. J Polym Sci, Part B: Polym Phys 1992, 30, 1021.
4. Won, H. J.; Chan, D. P.; Moo, S. L. Polymer 1996, 37, 1709.
5. Majumdar, B.; Keskkula, J.; Paul, D. R. Polymer 1994, 35, 3164.
6. Carrot, C.; Guillet, J.; May, J. F. Plast, Rubber Compos Proc Appl 1991, 16, 61.
7. Byung, K. K.; Yong, M. L. Polymer 1993, 34, 2075.
8. Horak, Z.; Krulis, Z.; Baldrian, J.; Fortelny, I. Polym Networks Blends 1997, 7, 43.

9. Sathe, S.; Rao, G. S. S.; Rao, K. V.; Devi, S. Polym Eng Sci 1996, 36, 2443.
10. Zhang, X. M.; Li, X. L.; Wang, D. M.; Yin, Z. H.; Yin, J. H. J Appl Polym Sci 1997, 64, 1489.
11. Valenza, A.; Gueskens, G.; Spadaro, G. Eur Polym J 1997, 33, 957.
12. Chang, D. Y.; Kuo, W. F.; Chang, F. C. Polym Networks Blends 1994, 4, 157.
13. Kim, J. K.; Lee, H. Polymer 1996, 37, 305.
14. Nikos, K. K.; Dimitrios, S. S.; Joannis, K. K. Polymer 1996, 37, 3387.
15. Lotz, B.; Kovacs, A. J. Polym Prepr 1969, 10, 820.
16. Robitaille, V.; Prud omme, J. Macromolecules 1983, 16, 665.
17. Aref-Azar, A.; Hay, J. N.; Marsden, B.; Neil, W. J Polym Sci, Polym Phys 1980, 18, 637.
18. Ghijsels, A.; Groesbeek, N.; Yip, C. W. Polymer 1983, 23, 1913.
19. Klemmer, N.; Jungrickel, B.-J. Colloid Polym Sci 1984, 262, 381.
20. Frensch, H.; Jungnickel, B. J. Colloid Polymer Sci 1989, 28, 2267.
21. Ikkala, O. T.; Holsti-Miettinen, R. M.; Seppala, J. J Appl Polym Sci 1993, 49, 65.
22. Radusch, H.-J.; Androsch, R. Angew Makrom Chem 1994, 214, 179.
23. Stolp, M.; Androsch, R.; Radrsch, H.-J. Polym Networks Blends 1996, 4, 1141.
24. Pound, G. M.; Lamer, V. K. J Am Chem Soc 1952, 74, 2323.
25. Taylor, G. I. Proc R Soc London 1934, A146, 501.
26. Taylor, G. I. Proc R Soc London 1932, A138, 41.
27. Todita, N. Rubber Chem Technol 1977, 50, 292.
28. Illing, G. in Polymer Blends, Processing, Morphology and Properties; Martuselli, E.; Palumbo, R.; Kryszewski, M., Eds.; Plenum Press: New York, 1980; p. 167.